CHEMMEDCHEM

CHEMISTRY ENABLING DRUG DISCOVERY

Accepted Article

Title: Synthesis and preliminary evaluation of [11C]GNE-1023 as a novel potent PET probe for imaging leucine-rich repeat kinase 2 (LRRK2) in Parkinson's disease

Authors: Zhen Chen, Tuo Shao, Wei Gao, Hualong Fu, Thomas Lee Collier, Jian Rong, Xiaoyun Deng, Qingzhen Yu, Xiaofei Zhang, April T. Davenport, James B. Daunais, Hsiao-Ying Wey, Yihan Shao, Lee Josephson, Wen-Wei Qiu, and Steven Liang

To be cited as: *ChemMedChem* 10.1002/cmdc.201900321

Link to VoR: http://dx.doi.org/10.1002/cmdc.201900321

A Journal of

ChemPubSoc Europe

WILEY-VCH

www.chemmedchem.org

WILEY-VCH

COMMUNICATION

Synthesis and preliminary evaluation of [^{11}C]GNE-1023 as a novel potent PET probe for imaging leucine-rich repeat kinase 2 (LRRK2) in Parkinson's disease

Zhen Chen,[a]+ Tuo Shao,[a]+ Wei Gao[b] Hualong Fu,[a] Thomas Lee Collier,[a] Jian Rong,[a] Xiaoyun Deng,[a] Qingzhen Yu,[a] Xiaofei Zhang,[a] April T. Davenport,[c] James B. Daunais,[c] Hsiao-Ying Wey,[d] Yihan Shao,[e] Lee Josephson,[a] Wen-Wei Qiu*[b] and Steven Liang*[a]

[a] Dr. Z. Chen, Dr. T. Shao, Dr. H. Fu, Dr T. L. Collier, Dr. J. Rong, Dr. X. Deng, Dr. Q. Yu, Dr. X. Zhang, Prof. Dr. L. Josephson, Prof. Dr. S. Liang
Department of Radiology, Division of Nuclear Medicine and Molecular Imaging
Massachusetts General Hospital and Harvard Medical School
55 Fruit Street, Boston, Massachusetts 02114, United States
E-mail: liang.steven@mgh.harvard.edu

[b] W. Gao, Prof. Dr. W.-W. Qiu
Shanghai Engineering Research Center of Molecular Therapeutics and New Drug Development, School of Chemistry and Molecular Engineering
East China Normal University
500 Dongchuan Road, Shanghai, 200241, China
E-mail: wwqiu@chem.ecnu.edu.cn

[c] A. T. Davenport, Prof. Dr. J. B. Daunais
Department of Physiology and Pharmacology
Wake Forest School of Medicine
Winston Salem, North Carolina 27157, United States

[d] Prof. Dr. H.-Y. Wey
Athinoula A Martinos Center for Biomedical Imaging, Department of Radiology
Massachusetts General Hospital and Harvard Medical School
55 Fruit Street, Boston, Massachusetts 02114, United States

[e] Prof. Dr. Y. Shao
Department of Chemistry and Biochemistry
University of Oklahoma
Norman, Oklahoma 73019, United States

+ These authors contribute equally to this work.

Supporting information for this article is given via a link at the end of the document.((Please delete this text if not appropriate))

Abstract: Leucin-rich repeat kinase 2 (LRRK2) is a large protein that is involved in the pathogenesis of Parkinson's disease (PD). It has been demonstrated that LRRK2 mutations mainly confers PD, which bring about increased kinase activity of LRRK2. As a consequence, selective inhibition of LRRK2 may help to recover the normal functions of LRRK2, and thereafter serve as an alternatively promising therapeutic target for PD treatment. The mapping of LRRK2 with PET studies allows a deep understanding of PD and other LRRK2-related disorders, as well as helps to validate and translate novel LRRK2 inhibitors. However, to date no LRRK2 PET probes have been reported in the primary literature. In this study, we present a facile synthesis and preliminary evaluation of [^{11}C]GNE-1023 as a novel potent PET probe for LRRK2 imaging in PD. [^{11}C]GNE-1023 was synthesized in good radiochemical yield (10% non-decay corrected RCY), excellent radiochemical purity (>99%) and high molar activity (>37 GBq / μmol). Excellent in vitro binding specificity of [^{11}C]GNE-1023 towards LRRK2 was demonstrated in cross species studies, including rat and nonhuman primate brain tissues by autoradiography experiments. Subsequent whole-body biodistribution studies indicated limited brain uptake and urinary and hepatobiliary elimination of this radioligand. This study may pave the way for the further development of a new generation of LRRK2 PET probes.

Parkinson's disease (PD) is one of the most prevailing neurodegenerative disorders in the central nervous system (CNS), which affects approximately 10% of the population over the age of 60.[1] Despite great efforts devoted to the investigation of PD pathogenesis, currently the detailed etiology still remains unclear, and no effective therapy has been approved to prevent, cure and slow the PD progress. In the past decades, the leucine-rich kinase 2 (LRRK2) gene has been established as being involved in PD pathogenesis. The LRRK2 gene is a large protein comprising a central enzymatic core and a diversity of protein-protein interaction domains[2-4], and is widely distributed throughout the CNS and other peripheral organs. While, in rodent brain, LRRK2 exhibits regional heterogeneity in expression levels, and the highest levels are found in the striatum, cerebral cortex and hippocampus,[5] in human brain, LRRK2 is mostly expressed in the putamen and substantia nigra.[6] LRRK2 is also expressed in the lung, kidney, liver and heart.[7] It has been demonstrated that mutations of LRRK2 are associated with PD, which are linked to ~10% of familial cases and 2% of sporadic cases.[6, 8-10] Numerous in vitro and in vivo studies indicated that multiple mutations of LRRK2 can lead to increased kinase activity, and the most common mutation is dominated by a G2019S variant.[11-16] As a consequence, selective inhibition of LRRK2 may help to recover the normal functions of LRRK2, and thereafter serve as a promising therapeutic target for PD treatment.[17-18] In the last decade, several LRRK2 inhibitors including GNE-1023, GNE-7915, GNE-0877, GNE-9605, PF-06447475 and MLi-2 have been reported (Figure 1).[19-23] Among these, GNE-1023 [3-methoxy-4-((4-(methylamino)-5-(trifluoromethyl)pyrimidin-2-

yl)amino)phenyl)-(morpholino)meth-anone] was identified as a potent, selective and brain-penetrant LRRK2 inhibitor (IC_{50} = 9 nM), which efficiently reduced the kinase activity of LRRK2 in HEK293 cell assays as well as in the bacterial artificial chromosome (BAC) transgenic mouse brain overexpressing G2019S mutant LRRK2.[24] Particularly noteworthy is that this compound and GNE-1023 entail a phenolic methyl group, which would allow a facile labeling with carbon-11 for PET imaging studies.[25]

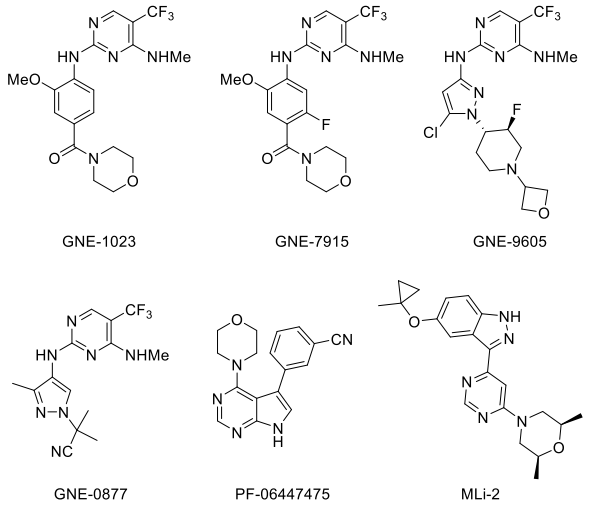

Figure 1. Structures of reported LRRK2 inhibitors.

As a non-invasive and highly-sensitive molecular imaging tool, positron emission tomography (PET) has been widely used to probe in vivo biological processes under normal or disease conditions.[26-28] PET studies of LRRK2 would enable a deep understanding of PD and other LRRK2-related disorders, as well as help to validate and translate novel LRRK2 inhibitors. Despite these benefits, to date no LRRK2-specific PET probe has been reported in the primary literature. Therefore, an unmet clinical need of LRRK2 imaging probes together with therapeutic potential of LRRK2-related pharmacotherapy represents an intensive motivation in the field. In 2013, several ^{11}C- or ^{18}F-labeled LRRK2 inhibitors based on GNE-1023 and its close analogs were disclosed in a patent of Genentech with limited biological information.[29] To date, there is only one LRRK2 PET ligand [^{11}C]HG-10-102-01 developed by Zheng and co-workers in 2017 from the primary literature.[30] However, no biological data was reported for this ligand. It is worth noting that, during the review of this manuscript, Ding et al reported two ^{18}F-labeled LRRK2 inhibitors in a conference proceeding and biological evaluation is underway.[31] Here we present an efficient synthesis and preliminary in vitro and in vivo evaluation of [^{11}C]GNE-1023 as a potential PET probe for LRRK2 imaging in PD.

We performed the synthesis of LRRK2 inhibitor **6** (GNE-1023) and its corresponding demethylated precursor **7** using modified procedures as depicted in Scheme 1. Briefly, commercially available starting material 3-methoxy-4-nitrobenzoic acid **1** was activated with $SOCl_2$, and then coupled with morpholine to deliver amide **2** in 96% yield over two steps. Iron-mediated reduction of the nitro group in **2** occurred smoothly to yield aniline derivative **3** with high efficiency in the presence of acetic acid. In parellel, amination reaction of commercially available starting material 2,4-dichloro-5-(trifluoromethyl)pyrimidine **4** with methylamine readily proceeded under basic conditions to generate compound **5** in moderate yield (40%). The desired LRRK2 inhibitor **6** was obtained by S_N2 displacement reaction of **5** with aniline **3** at 185 °C in a co-solvent of trifluoroacetic acid (TFA) and butanol (n-BuOH). Ultimately, compound **6** was swiftly demethylated by boron tribromide (BBr_3) to deliver the corresponding phenolic precursor **7** in 69% yield for subsequent radiosynthesis.

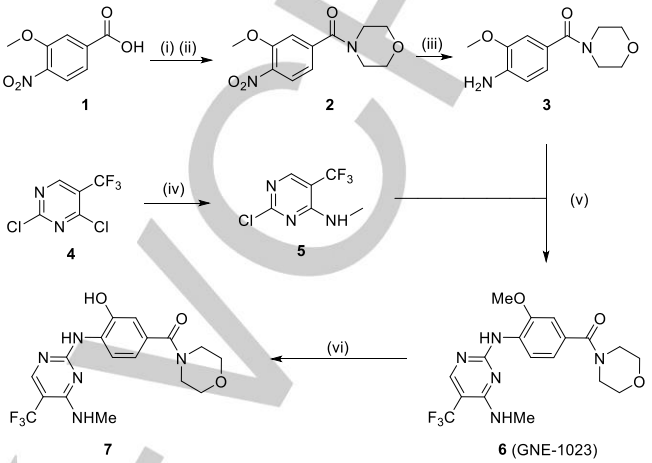

Scheme 1. Synthesis of LRRK2 inhibitor **6** (GNE-1023) and its demethylated precursor **7.** (i) $SOCl_2$, DME, reflux, 6 h; (ii) morpholine, 3-methoxy-4-nitrobenzoyl chloride, DIPEA, THF, 0 °C, 1h, 96% over two steps; (iii) Fe, AcOH, r.t., 3 h, 90%; (iv) $MeNH_2$, Et_3N, MeOH, r.t., 12 h, 40%; (v) TFA, 2-butyl alcohol, 185 °C, 12 h, 31%; (vi) BBr_3, DCM, r.t., 12 h, 69%. DME = 1,2-dimethoxyethane, DIPEA = *N*,*N*-diisopropylethylamine, THF = tetrahydrofuran, TFA = trifluoroacetic acid, DCM = dichloromethane.

Attributed to the existence of methoxy group in GNE-1023, radiosynthesis of compound **6** can be conveniently performed using [^{11}C]CH_3I from its corresponding phenolic precursor **7**. All processes from radiolabeling, purification and formulation of [^{11}C]**6** were carried out with an automated synthetic module (TRACERlab FX MeI, GE). The radiosynthesis of [^{11}C]**6** was conducted by reacting **7** with [^{11}C]CH_3I at 80 °C for 5 min in the presence of NaOH in *N,N*-dimethylformide (DMF) (Scheme 2A). It should be noted that the amount of precursor had a profound effect on the RCY of this radiolabeling. While desired product was generated with 1.0 mg precursor (Scheme 2A; entries 1 and 2), increasing amount of precursor remarkably improved the reaction yield (entries 3 and 4). In particular, a quantitative radiochemical conversion with high isolated radiochemical yield (entry 4) was achieved when 1.6 mg precursor was used. The reaction mixture was purified with semi-preparative reverse high-performance liquid chromatography (HPLC) to give [^{11}C]**6**, which was subsequently formulated in saline containing 10% of ethanol. Ultimately, [^{11}C]**6** was obtained in an average of 10% non-decay corrected radiochemical yield (RCY) relative to starting [^{11}C]CO_2 at the end of synthesis (EOS) with excellent radiochemical purity (>99%) and high molar activity (>37 GBq/μmol). Average synthetic time was 42 minutes. In addition, no radiolysis was observed for [^{11}C]**6** up to 100 min after formulation (Scheme 2B).

Lipophilicity is an emprical parameter to predict the ability of a candidate to cross the blood-brain barrier (BBB), and favors a range of 1.0-3.5.[32-34] The lipophilicity of [^{11}C]**6** (log*D*) was determined to be 2.93 ± 0.02 through liquid-liquid partition between PBS and *n*-octanol, which is also well-known as the

'shake flask method'.[35] This result indicated that [^{11}C]**6** possesses a high possibility to penetrate the BBB.

(A) Optimization of reaction parameters for radiosynthesis of [^{11}C]**6**

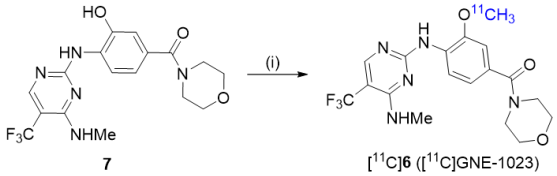

7 [^{11}C]**6** ([^{11}C]GNE-1023)

Entry	Precursor	Base (x equiv)	RCY[a]
1	1.0 mg	TBAOH (0.7)	trace
2	1.0 mg	NaOH (0.7)	trace
3	1.2 mg	NaOH (0.7)	3%
4	1.6 mg	NaOH (1.0)	10%

(B) Stability of radioligand [^{11}C]**6**

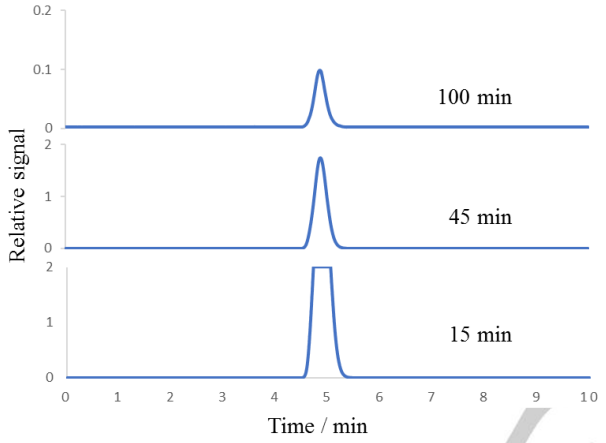

Scheme 2. (A) Optimization of reaction parameters for radiosynthesis of [^{11}C]**6**. (i) [^{11}C]MeI, DMF, 80 °C, 5min. [a] Non-decay corrected RCY relative to starting [^{11}C]CO_2. (B) Stability of radioligand [^{11}C]**6** in saline containing 10% of ethanol. HPLC conditions: Gemini® C18 column (3 x 150 mm, 5 µm); mobile phase: CH_3CN/H_2O + 0.1% Et_3N (v/v, 40/60); flowrate: 0.8 mL/min. TBAOH = tetrabutylammonium hydroxide, DMF = *N,N*-dimethylformide.

With radioligand [^{11}C]**6** in hand, we then carried out autoradiography studies in brain sections of Sprague Dawley rats (Figure 2) and non-human primates (Figure 3) to investigate in vitro binding specificity towards LRRK2. As shown in Figure 2, in rat brain sections, under baseline conditions, [^{11}C]**6** exhibited heterogeneous distribution of radioactivity with the highest level in hippocampus, followed by cerebral cortex and striatum, and the lowest level in cerebellum, which is consistent with the expression pattern of LRRK2 in rodents (Figure 2A and 2B). Pretreatment with PF-06447475, a commercially available LRRK2 inhibitor, conferred a significant reduction of the bound radioactivity (ca. 50%) in all regional brains, suggesting excellent in vitro binding specificity of [^{11}C]**6** in rat brain towards LRRK2 (Figure 2C and 2D). The high level of in vitro specific binding of [^{11}C]**6** to LRRK2 was also demonstrated in non-human primate (NHP, rhesus monkey) brain sections, with 49% and 47% reduction of radioactivity in cortex (including all cortical areas, lateral and medial orbital cortex) and caudate nucleus, respectively, under blocking conditions (Figure 3).

The uptake, biodistribution and clearance of radioligand [^{11}C]**6**

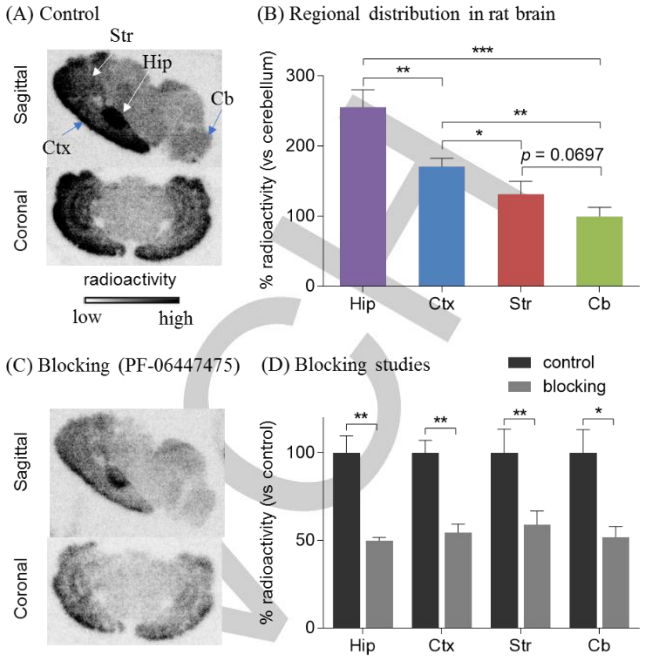

Figure 2. In vitro autoradiography of [^{11}C]**6** in rat brain sections. (A) Brain sections were treated with [^{11}C]**6**; (B) Regional radioactivity distribution of [^{11}C]**6** in rat brain (baseline). The data were normalized to % of radioactivity vs that in cerebellum (n = 3); (C) Brain sections were pre-treated with PF-06447475 (10 µM), a known LRRK2 inhibitor, followed by [^{11}C]**6**; (D) Blocking studies. The data were normalized to % of radioactivity vs control (n = 3). Hip = hippocampus; Ctx = cerebral cortex; Str = striatum; Cb = cerebellum. Asterisks indicate statistical significance. *p < 0.05, **p ≤0.01, and ***p ≤0.001.

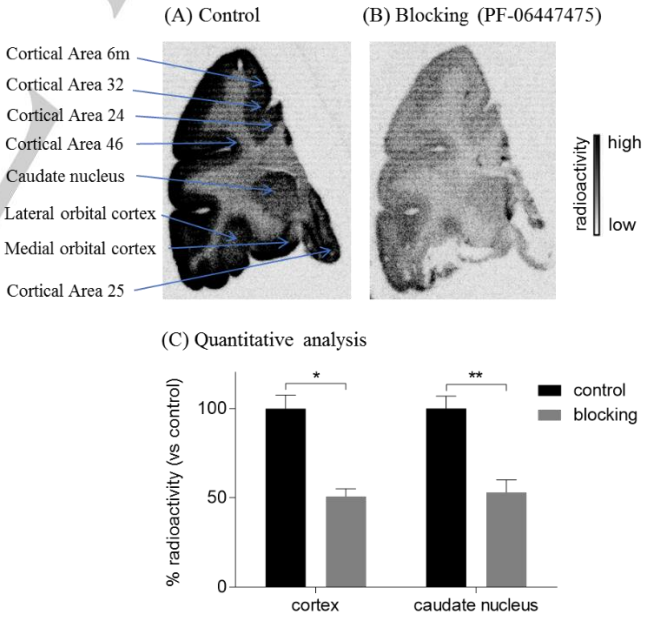

Figure 3. In vitro autoradiography of [^{11}C]**6** in rhesus monkey brain sections. (A) Brain sections were treated with [^{11}C]**6**; (B) Brain sections were pre-treated with PF-06447475 (10 µM), a known LRRK2 inhibitor, followed by [^{11}C]**6**; (C) Quantification of the radioactivity of [^{11}C]**6** in cortex (including all cortical areas, lateral and medial orbital cortex) and caudate nucleus under control and blocking conditions. The data were normalized to % of radioactivity vs control (n = 3). Asterisks indicate statistical significance. *p < 0.05, and **p ≤0.01.

was evaluated by performing whole-body ex vivo biodistribution studies in mice at four time points (5, 15, 30 and 60 min) after intravenous tracer injection. As illustrated in Figure 4 and Table

S1 in the Supporting Information, radioligand [^{11}C]**6** exhibited limited brain uptake (1.85% ID/g, injected dose per gram of wet tissue at 5 min), suggesting insufficient BBB permeability in rodents. High uptake (>5% ID/g) showed up in multiple peripheral organs including heart, lungs, liver, pancreas, kidneys, small intestine and stomach, at 5 min, which is in line with the LRRK2 peripheral expression. While the radioactivity in most organs was rapidly washed out after 5 min, bound signal in small intestine reached a plateau at 30 min prior to efficient clearance. At 60 min, high radioactivity was retained in liver, kidneys and small intestine. These results indicated that radioligand was eliminated through both urinary and hepatobiliary pathways.

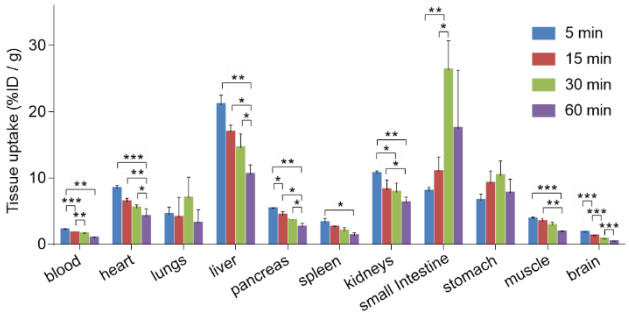

Figure 4. Whole-body ex vivo biodistribution studies of [^{11}C]**6** in mice at four different time points (5, 15, 30 and 60 min) post tracer injection. Data are expressed as % ID/g (mean ± SD; n = 4). Asterisks indicate statistical significance. $^{*}p < 0.05$, $^{**}p \leq 0.01$, and $^{***}p \leq 0.001$.

In this study, we have efficiently synthesized a novel LRRK2 PET probe [^{11}C]**6** ([^{11}C]GNE-1023) in good radiochemical yield, excellent radiochemical purity and high molar activity. Autoradiography studies demonstrated excellent in vitro specific binding of [^{11}C]**6** to LRRK2 in rat and NHP brain sections. The whole-body ex vivo bio-distribution studies exhibited limited brain accumulation, and excretion pathway, specifically urinary and hepatobiliary elimination for [^{11}C]**6** in mice. Although [^{11}C]**6** showed limited brain uptake in rodents, given favorate ADME profile of **6** in MDCK-MDR1 human Pgp transfected cell lines (P_{app} A-B, 18.2 x 10^{-6} cm/s; Efflux ratio, B-A/A-B, 1.2),[21] species difference in BBB permeability may exist between rodents and NHPs.[36-40] Further in vivo evaluation in higher species and medicinal chemistry modification based on [^{11}C]**6** scaffold to improve the BBB permeability is ongoing in our program.

Experiment Sections

The general procedure for experimental section was described previously[41] with minor modification in this work. All the chemicals employed in the synthesis were purchased from commercial vendors and used without further purification. Thin-layer chromatography (TLC) was conducted with 0.25 mm silica gel plates ($^{60}F_{254}$) and visualized by exposure to UV light (254 nm) or stained with potassium permanganate. Flash column chromatography was performed using silica gel (particle size 0.040-0.063 mm). Nuclear magnetic resonance (NMR) spectra were obtained either on a Bruker spectrometer 300, 400 or 500 MHz. Chemical shifts (δ) are reported in ppm, and coupling constants are reported in Hertz. The multiplicities are abbreviated as follows: s = singlet, d = doublet, t = triplet, q = quartet, quint = quintet, sext = sextet, sept = setpet, m = multiplet, br = broad signal, dd = doublet of doublets. Molar activity determinations are reported at the end of synthesis, unless otherwise stated. The animal experiments were approved by the Institutional Animal Care and Use Committee of Massachusetts General Hospital (OLAW Assurance D16-00361). CD-1 mice (female; 7 weeks, 22-24 g) were kept on a 12 h light/12 h dark cycle and were allowed food and water *ad libitum*.

(3-methoxy-4-nitrophenyl)(morpholino)methanone (2): Under nitrogen atmosphere, to a 100 mL two-neck flask containing a condenser was added 3-methoxy-4-nitrobenzoic acid **1** (1 g, 5.0 mmol), 1,2-dimethoxyethane (DME, 20 mL) and thionyl chloride ($SOCl_2$, 3 mL, 41 mmol). The resulting mixture was heated to 85 °C and stirred at the same temperature for 6 h until starting material **1** disappeared as monitored by TLC. Then the reaction mixture was allowed to cool to room temperature and evaporated to dryness under reduced pressure to give the crude 3-methoxy-4-nitrobenzoyl chloride, which was directly re-dissolved in dry tetrahydrofuran (THF, 20 mL). Under nitrogen atmosphere at 0 °C, *N*,*N*-diisopropylethylamine (DIPEA, 1.8 mL, 10 mmol) and morpholine (0.86 mL, 10 mmol) was successively added to the above solution. The resulting mixture was stirred at 0 °C for 1 h before water (200 mL) was added. After stirring for another 10 min, the aqueous phase was extracted with ethyl acetate (20 mL × 5). The organic phases were combined, washed with brine, dried over anhydrous Na_2SO_4, and then concentrated under reduced pressure. The residue was purified by a silica gel chromatography (PE / EA = 1 / 3) to yield the product as a yellow solid (1.28 g, 96% over two steps). ^{1}H NMR (500 MHz, DMSO) δ 7.93 (d, *J* = 8.2 Hz, 1H), 7.37 (s, 1H), 7.12 (d, *J* = 8.2 Hz, 1H), 3.95 (s, 3H), 3.70 – 3.51 (m, 6H), 3.30 (s, 2H). ^{13}C NMR (101 MHz, $CDCl_3$) δ 167.97, 153.18, 141.09, 140.06, 125.81, 118.37, 112.64, 66.71, 56.73.

(4-amino-3-methoxyphenyl)(morpholino)methanone (3): To a flask containing **2** (1 g, 3.76 mmol) and acetic acid (12 mL) was added iron powder (2.73 g, 48.8 mmol, 13 equiv). Under nitrogen atmosphere, the resulting mixture was stirred at room temperature for 3 h until **2** disappeared as monitored by TLC. The reaction mixture was filtered, and the filtrate was concentrated *in vacuo*. The residue was purified by a silica gel chromatography (CH_2Cl_2 / MeOH = 40 / 1) to afford the desired product as a white solid (800 mg, 90%). ^{1}H NMR (500 MHz, DMSO) δ 6.85 (s, 1H), 6.80 (dd, *J* = 8.0, 1.3 Hz, 1H), 6.62 (d, *J* = 8.0 Hz, 1H), 5.14 (s, 2H), 3.78 (s, 3H), 3.61 – 3.55 (m, 4H), 3.53 – 3.47 (m, 4H). ^{13}C NMR (101 MHz, $CDCl_3$) δ 171.00 (s), 146.60 (s), 138.65 (s), 123.86 (s), 120.93 (s), 113.22 (s), 110.24 (s), 66.86 (s), 55.48 (s).

2-chloro-N-methyl-5-(trifluoromethyl)pyrimidin-4-amine (5): To a solution of 2,4-dichloro-5-(trifluoromethyl)pyrimidine **4** (2 g, 9.2 mmol) in MeOH (35 mL) was successively added triethylamine (Et_3N, 1.31 mL, 9 mmol) and methylamine (2.0 M in MeOH, 5 mL, 10 mmol) at 0 °C. The resulting mixture was allowed to warm to room temperature and stirred at the same temperature for 12 h until **4** disappeared as monitored by TLC. The reaction mixture was then evaporated to dryness *in vacuo*, and the residue was purified on a silica gel chromatography (PE / EA = 30 / 1) to give the product as a white solid (780 mg, 40%). ^{1}H NMR (500 MHz, DMSO) δ 8.37 (s, 1H), 7.92 (s, 1H), 2.89 (d, *J* = 4.4 Hz, 3H). ^{13}C NMR (101 MHz, $CDCl_3$) δ 163.77 (s), 159.71 (s), 154.79 (q, *J* = 5.1 Hz), 123.66(q, *J* = 2.7 Hz), 106.00(q, *J* = 0.33 Hz) 28.41 (s).

(3-methoxy-4-((4-(methylamino)-5-(trifluoromethyl)pyrimi-din-2-yl)a-mino)phenyl)(morpholino)methanone (6, GNE-1023): To a high-pressure reactor was successively added **3** (380 mg, 1.6 mmol), **5** (400 mg, 1.9 mmol), 2,2,2-trifluoroacetic acid (TFA, 1 mL) and 2-butyl alcohol (35 mL). The resulting mixture was heated to 185 °C and stirred at the same temperature for 12 h before cooling to room temperature. The reaction mixture was then evaporated to dryness *in vacuo*, and the residue was purified by a silica gel chromatography (CH_2Cl_2 / MeOH = 60 / 1) to deliver the product as a white solid (242 mg, 31%). Melting point = 177 –

178 °C. ^{1}H NMR (300 MHz, DMSO) δ 8.32 (d, *J* = 8.2 Hz, 1H), 8.19 (s, 1H), 8.08 (s, 1H), 7.23 (d, *J* = 3.2 Hz, 1H), 7.08 (d, *J* = 1.6 Hz, 1H), 7.02 (dd, *J* = 8.2, 1.7 Hz, 1H), 3.90 (s, 3H), 3.75 – 3.39 (m, 8H), 2.92 (d, *J* = 3.1 Hz, 3H). ^{13}C NMR (75 MHz, DMSO) δ 169.33, 161.03, 158.89, 154.75 (d, *J* = 5.3 Hz),148.77, 130.03, 129.93, 125.28 (q, *J* = 269.5 Hz),.119.98, 119.75, 110.42, 98.61 (q, *J* = 31.9 Hz), 66.55, 56.48, 28.49.

(3-hydroxy-4-((4-(methylamino)-5-(trifluoromethyl)pyrimi-din-2-yl)amino)phenyl)(morpholino)methanone (7): To a solution of **6** (200 mg, 0.49 mmol) in dry CH_2Cl_2 (10 mL) was added boron tribromide (1.0 M in CH_2Cl_2, 2 mL, 2 mmol). The resulting mixture was allowed to warm to room temperature and stirred at the same temperature for 12 h before saturated aqueous $NaHCO_3$ solution (15 mL) was added. After stirring for an additional 5 min, the reaction mixture was transferred to a separatory funnel, and the organic layer was successively separated, washed with brine, dried over anhydrous Na_2SO_4, and then evaporated to dryness *in vacuo*. The residue was purified by a silica gel chromatography (CH_2Cl_2 / MeOH = 30 / 1) to provide the product as a white solid (135 mg, 69%). Melting point = 270 – 271 °C. ^{1}H NMR (300 MHz, DMSO) δ 10.42 (s, 1H), 8.21 – 8.12 (m, 3H), 7.24 (d, *J* = 4.2 Hz, 1H), 6.98 – 6.77 (m, 2H), 3.59 (s, 4H), 3.50 (s, 4H), 2.92 (d, *J* = 4.3 Hz, 3H). ^{13}C NMR (75 MHz, DMSO) δ 169.38, 160.98, 158.88, 154.64 (q, *J* = 5.6 Hz), 146.85, 129.99, 129.33, 125.27 (q, *J* = 269.5 Hz), 120.13, 118.82, 114.61, 98.44 (d, *J* = 31.7 Hz), 66.60, 28.50.

Radiosynthesis of [^{11}C]6 ([^{11}C]GNE-1023). The general procedure for radiolabeling with [^{11}C]CH_3I was described previously with minor modification in this work.[42] Briefly, [^{11}C]CH_3I was transferred under helium gas with heating into a reaction vessel containing the phenolic precursor **7** (1.6 mg), NaOH (4 μL, 1.0 M), and anhydrous DMF (300 μL). After the radioactivity reached a plateau during transfer, the reaction vessel was warmed to 80 °C and maintained for 5 min. CH_3CN/H_2O + 0.1% Et_3N (v/v, 50/50, 1.5 mL) was added to the reaction mixture, which was then injected to a semipreparative HPLC system. HPLC purification was completed on a X-select® C18 column (10 mm i.d. × 250 mm) using a mobile phase of CH_3CN/H_2O + 0.1% Et_3N (v/v, 50/50) at a flow rate of 5.0 mL/min. The retention time for **[^{11}C]6** was 8.7 min. The radioactive fraction corresponding to the desired product was collected in a sterile flask, diluted with 30 mL of water, trapped on a Sep-Pak light C18 cartridge. After washing with 10 mL of water to remove CH_3CN residue, the product was washed out from the cartridge with 1 mL of ethanol, and formulated with 10 mL of PBS-buffered saline. The total synthetic time was ~42 min from the end of bombardment. Radiochemical and chemical purity were measured by analytical HPLC (Gemini® C18 column, 3 mm i.d. × 150 mm, UV at 254 nm; CH_3CN/H_2O + 0.1% Et_3N (v/v, 40/60) at a flow rate of 0.8 mL/min, retention time: 4.9 min). The identity of product was confirmed by the co-injection with unlabeled compound **6**. Radiochemical yield was 10% non-decay-corrected based on [^{11}C]CO_2 with >99% radiochemical purity, and the molar activity was greater than 37.0 GBq/μmol (1.0 Ci/μmol).

Measurement of the lipophilicity: The general procedure for lipophilicity measurement was described previously[41, 43] with minor modification in this work. Briefly, the measurement of Log*D* value was carried out by mixing [^{11}C]**6** (radiochemical purity >99%) with *n*-octanol (3.0 g) and PBS (0.1 M, 3.0 g) in a test tube. Both *n*-octanol and PBS were pre-saturated with each other prior to use. The tube was first vortexed for 5 min, followed by centrifugation (~3500-4000 rpm) for an additional 5 min. PBS and n-octanol (0.60 mL each) were aliquoted, weighted and the radioactivity in each component was measured using a Cobra Model 5002/5003 autogamma counter. The Log*D* was determined by Log [ratio of radioactivity between the n-octanol and PBS solutions] (n = 3).

In vitro autoradiography: The general procedure for lipophilicity measurement was described previously.[44] Brain sections of rat and rhesus monkey were pre-incubated with Tris-HCl buffer (50 mM), $MgCl_2$ (1.2 mM) and $CaCl_2$ (2 mM) solution for 20 min at ambient temperature, followed by incubation with [^{11}C]**6** (0.48 nM). For blocking studies, PF-06447475 (10 μM), a known LRRK2 inhibitor, was added to incubation solution in advance to determine the specificity of radioligand binding. After incubation, brain sections were rinsed with ice-cold buffer three times for 2 min, dipped in cold distilled water for 10 seconds. The brain sections were dried with cold air, then placed on imaging plates (BAS-MS2025, GE Healthcare, NJ, USA) for optimized contact periods. Autoradiograms were obtained and regions of interest (ROIs) were carefully drawn with the reference of naked-eye observation. Radioactivity was measured by an Amersham Typhoon 5 analyzer system and normalized to % of radioactivity vs control.

Whole-body ex vivo biodistribution studies: The general procedure for ex vivo biodistribution studies was described previously[41, 43] with minor modification in this work. Briefly, a solution of [^{11}C]**6** (50 μCi / 100 μL) was injected into CD-1 mice via tail vein. These mice (each time point n = 4) were sacrificed at 5, 15, 30 and 60 min post tracer injection. Major organs, including whole brain, heart, liver, lungs, spleen, kidneys, small intestine (including contents), muscle, pancreas, stomach and blood were quickly harvested and weighed. The radioactivity present in these tissues was measured using a Cobra Model 5002/5003 autogamma counter, and all radioactivity measurements were automatically decay corrected based on the half-life of carbon-11. The results are expressed as the percentage of injected dose per gram of wet tissue (% ID/g).

Statistical Analysis: Statistical analysis was performed by a student's two-tailed t-test, and asterisks were used to indicate statistical significance: $^{*}p < 0.05$, $^{**}p \leq 0.01$, and $^{***}p \leq 0.001$.

Acknowledgements

We thank Elijahu Livni (Nuclear Medicine and Molecular Imaging, Radiology, MGH and Harvard Medical School) for advice in the radiosynthesis and Professor Thomas J. Brady (Nuclear Medicine and Molecular Imaging, Radiology, MGH and Harvard Medical School) for helpful discussion. We also thank Genentech for providing the material, helpful discussion and support to publish our preliminary results. Financial support from NIH grants (NIAAA AA019431 to J.B.D.and NIAAA AA014106 to David P. Friedman) is gratefully acknowledged.

Conflict of interest

The authors declare no conflict of interest.

Keywords: Parkinson's disease • leucine-rich repeat kinase 2 • positron emission tomography • carbon-11 • GNE-1023

References:

[1] A. J. Lees, J. Hardy, T. Revesz, *Lancet* **2009**, *373*, 2055-2066.

[2] M. Funayama, K. Hasegawa, H. Kowa, M. Saito, S. Tsuji, F. Obata, *Ann. Neurol.* **2002**, *51*, 296-301.

[3] A. B. West, D. J. Moore, S. Biskup, A. Bugayenko, W. W. Smith, C. A. Ross, V. L. Dawson, T. M. Dawson, *Proc. Natl. Acad. Sci. USA* **2005**, *102*, 16842-16847.

[4] I. F. Mata, W. J. Wedemeyer, M. J. Farrer, J. P. Taylor, K. A. Gallo, *Trends Neurosci.* **2006**, *29*, 286-293.

[5] J.-M. Taymans, C. Van den Haute, V. Baekelandt, *J. Neurochem.* **2006**, *98*, 951-961.

[6] A. Zimprich, S. Biskup, P. Leitner, P. Lichtner, M. Farrer, S. Lincoln, J. Kachergus, M. Hulihan, R. J. Uitti, D. B. Calne, A. J. Stoessl, R. F. Pfeiffer, N.

Patenge, I. C. Carbajal, P. Vieregge, F. Asmus, B. Müller-Myhsok, D. W. Dickson, T. Meitinger, T. M. Strom, Z. K. Wszolek, T. Gasser, *Neuron* **2004**, *44*, 601-607.

[7] J. Miklossy, T. Arai, J.-P. Guo, A. Klegeris, S. Yu, E. G. McGeer, P. L. McGeer, *J. Neuropathol. Exp. Neurol.* **2006**, *65*, 953-963.

[8] R. Krüger, *BMC Med.* **2008**, *6*, 33.

[9] P. N. Gandhi, S. G. Chen, A. L. Wilson-Delfosse, *J. Neurosci. Res.* **2009**, *87*, 1283-1295.

[10] E. Greggio, M. R. Cookson, *ASN Neuro* **2009**, *1*, AN20090007.

[11] E. Greggio, S. Jain, A. Kingsbury, R. Bandopadhyay, P. Lewis, A. Kaganovich, M. P. van der Brug, A. Beilina, J. Blackinton, K. J. Thomas, R. Ahmad, D. W. Miller, S. Kesavapany, A. Singleton, A. Lees, R. J. Harvey, K. Harvey, M. R. Cookson, *Neurobiol. Dis.* **2006**, *23*, 329-341.

[12] M. R. Cookson, *Nat. Rev. Neurosci.* **2010**, *11*, 791-797.

[13] B. D. Lee, J.-H. Shin, J. P. VanKampen, L.; West, A. B.; Ko, H. S.; Lee, Y.-I.; Maguire-Zeiss, K. A.; Bowers, W. J.; Federoff, H. J.; Dawson, V. L.; Dawson, T. M. , *Nat. Med.* **2010**, *16*, 998-1000.

[14] D. Yang, W. W. Smith, Z. Liu, A. Ray, S. Hamamichi, G. A. Caldwell, K. A. Caldwell, B. Dae Lee, T. M. Dawson, V. L. Dawson, *Hum. Mol. Genet.* **2011**, *20*, 3933-3942.

[15] B. D. Lee, V. L. Dawson, T. M. Dawson, *Trends Pharmacol. Sci.* **2012**, *33*, 365-373.

[16] I. N. Rudenko, R. Chia, M. R. Cookson, *BMC Med.* **2012**, *10*, 20.

[17] R. E. Drolet, J. M. Sanders, J. T. Kern, *J. Neurogenet.* **2011**, *25*, 140-151.

[18] F. Atashrazm, N. Dzamko, *Clin. Pharmacol.* **2016**, *8*, 177-189.

[19] H. G. Choi, J. Zhang, X. Deng, J. M. Hatcher, M. P. Patricelli, Z. Zhao, D. R. Alessi, N. S. Gray, *ACS Med. Chem. Lett.* **2012**, *3*, 658-662.

[20] A. A. Estrada, B. K. Chan, C. Baker-Glenn, A. Beresford, D. J. Burdick, M. Chambers, H. Chen, S. L. Dominguez, J. Dotson, J. Drummond, M. Flagella, R. Fuji, A. Gill, J. Halladay, S. F. Harris, T. P. Heffron, T. Kleinheinz, D. W. Lee, C. E. L. Pichon, X. Liu, J. P. Lyssikatos, A. D. Medhurst, J. G. Moffat, K. Nash, K. Scearce-Levie, Z. Sheng, D. G. Shore, S. Wong, S. Zhang, X. Zhang, H. Zhu, Z. K. Sweeney, *J. Med. Chem.* **2014**, *57*, 921-936.

[21] A. A. Estrada, X. Liu, C. Baker-Glenn, A. Beresford, D. J. Burdick, M. Chambers, B. K. Chan, H. Chen, X. Ding, A. G. DiPasquale, S. L. Dominguez, J. Dotson, J. Drummond, M. Flagella, S. Flynn, R. Fuji, A. Gill, J. Gunzner-Toste, S. F. Harris, T. P. Heffron, T. Kleinheinz, D. W. Lee, C. E. Le Pichon, J. P. Lyssikatos, A. D. Medhurst, J. G. Moffat, S. Mukund, K. Nash, K. Scearce-Levie, Z. Sheng, D. G. Shore, T. Tran, N. Trivedi, S. Wang, S. Zhang, X. Zhang, G. Zhao, H. Zhu, Z. K. Sweeney, *J. Med. Chem.* **2012**, *55*, 9416-9433.

[22] M. J. Fell, C. Mirescu, K. Basu, B. Cheewatrakoolpong, D. E. DeMong, J. M. Ellis, L. A. Hyde, Y. Lin, C. G. Markgraf, H. Mei, M. Miller, F. M. Poulet, J. D. Scott, M. D. Smith, Z. Yin, X. Zhou, E. M. Parker, M. E. Kennedy, J. A. Morrow, *J.Pharmacol. Exp. Ther.* **2015**, *355*, 397-409.

[23] J. L. Henderson, B. L. Kormos, M. M. Hayward, K. J. Coffman, J. Jasti, R. G. Kurumbail, T. T. Wager, P. R. Verhoest, G. S. Noell, Y. Chen, E. Needle, Z. Berger, S. J. Steyn, C. Houle, W. D. Hirst, P. Galatsis, *J. Med. Chem.* **2015**, *58*, 419-432.

[24] Z. Sheng, S. Zhang, D. Bustos, T. Kleinheinz, C. E. Le Pichon, S. L. Dominguez, H. O. Solanoy, J. Drummond, X. Zhang, X. Ding, F. Cai, Q. Song, X. Li, Z. Yue, M. P. van der Brug, D. J. Burdick, J. Gunzner-Toste, H. Chen, X. Liu, A. A. Estrada, Z. K. Sweeney, K. Scearce-Levie, J. G. Moffat, D. S. Kirkpatrick, H. Zhu, *Sci. Trans. Med.* **2012**, *4*, 164ra161.

[25] X. Deng, J. Rong, L. Wang, N. Vasdev, L. Zhang, L. Josephson, S. H. Liang, *Angew. Chem. Int. Ed.* **2019**, *58*, 2580-2605.

[26] S. M. Ametamey, M. Honer, P. A. Schubiger, *Chem. Rev.* **2008**, *108*, 1501-1516.

[27] J. K. Willmann, N. van Bruggen, L. M. Dinkelborg, S. S. Gambhir, *Nat. Rev. Drug Discov.* **2008**, *7*, 591-607.

[28] P. W. Miller, N. J. Long, R. Vilar, A. D. Gee, *Angew. Chem., Int. Ed.* **2008**, *47*, 8998-9033.

[29] B. K. Chan, A. Estrada, J. Marik, Z. K. Sweeney, WO 2013079496, **2013**.

[30] M. Wang, M. Gao, Z. Xu, Q.-H. Zheng, *Bioorg. Med. Chem. Lett.* **2017**, *27*, 1351-1355.

[31] Y.-S. Ding, D. Clancy, G. Carlucci, N. Ramos, R. Jackson, F. Boada, S. Bruno, J. Ciaccio, *J. Nucl. Med.* **2019**, *60*, 1105.

[32] R. N. Waterhouse, *Mol. Imaging Biol.* **2003**, *5*, 376-389.

[33] S. Patel, R. Gibson, *Nucl. Med. Biol.* **2008**, *35*, 805-815.

[34] V. W. Pike, *Curr. Med. Chem.* **2016**, *23*, 1818-1869.

[35] *Test No. 107: Partition Coefficient (n-octanol/water): Shake Flask Method*, Organisation for Economic Cooperation and Development (OECD), Paris, **1995**.

[36] M. Bergström, K. J. Fasth, G. Kilpatrick, P. Ward, K. M. Cable, M. D. Wipperman, D. R. Sutherland, B. Långström, *Neuropharmacology* **2000**, *39*, 664-670.

[37] N. M. Rupniak, A. Fisher, S. Boyce, D. Clarke, A. Pike, D. O'Connor, A. Watt, *Behav. Pharmacol.* **2003**, *14*, 457-463.

[38] F. Yasuno, S. S. Zoghbi, J. A. McCarron, J. Hong, M. Ichise, A. K. Brown, R. L. Gladding, J. D. Bacher, V. W. Pike, R. B. Innis, *Synapse* **2006**, *60*, 510-520.

[39] S. Syvänen, Ö. Lindhe, M. Palner, B. R. Kornum, O. Rahman, B. Långström, G. M. Knudsen, M. Hammarlund-Udenaes, *Drug Metab. Dispos.* **2009**, *37*, 635-643.

[40] X. Chu, K. Bleasby, R. Evers, *Expert Opin. Drug Metab. Toxicol.* **2013**, *9*, 237-252.

[41] R. Cheng, W. Mori, L. Ma, M. Alhouayek, A. Hatori, Y. Zhang, D. Ogasawara, G. Yuan, Z. Chen, X. Zhang, H. Shi, T. Yamasaki, L. Xie, K. Kumata, M. Fujinaga, Y. Nagai, T. Minamimoto, M. Svensson, L. Wang, Y. Du, M. J. Ondrechen, N. Vasdev, B. F. Cravatt, C. Fowler, M.-R. Zhang, S. H. Liang, *J. Med. Chem.* **2018**, *61*, 2278-2291.

[42] Z. Chen, W. Mori, X. Deng, R. Cheng, D. Ogasawara, G. Zhang, M. A. Schafroth, K. Dahl, H. Fu, A. Hatori, T. Shao, Y. Zhang, T. Yamasaki, X. Zhang, J. Rong, Q. Yu, K. Hu, M. Fujinaga, L. Xie, K. Kumata, Y. Gou, J. Chen, S. Gu, L. Bao, L. Wang, T. L. Collier, N. Vasdev, Y. Shao, J.-A. Ma, B. F. Cravatt, C. Fowler, L. Josephson, M.-R. Zhang, S. H. Liang, *J. Med. Chem.* **2019**, *62*, 3336-3353.

[43] L. Wang, W. Mori, R. Cheng, J. Yui, A. Hatori, L. Ma, Y. Zhang, B. H. Rotstein, M. Fujinaga, Y. Shimoda, T. Yamasaki, L. Xie, Y. Nagai, T. Minamimoto, M. Higuchi, N. Vasdev, M.-R. Zhang, S. H. Liang, *Theranostics* **2016**, *6*, 1145-1159.

[44] Z. Chen, W. Mori, X. Zhang, T. Yamasaki, P. J. Dunn, G. W. Zhang, H. Fu, T. Shao, Y. Zhang, A. Hatori, L. Ma, M. Fujinaga, L. Xie, X. Deng, H. Li, Q. Yu, J. Rong, L. Josephson, J.-A. Ma, Y. Shao, S. Tomita, M. R. Zhang, S. H. Liang, *Eur. J. Med. Chem.* **2018**, *157*, 898-908.

WILEY-VCH

COMMUNICATION

Entry for the Table of Contents

Insert graphic for Table of Contents here. ((Please ensure your graphic is in **one** of following formats))

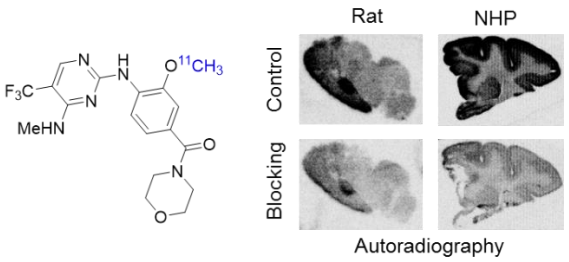

Insert text for Table of Contents here. ((The Table of Contents text should give readers a short preview of the main theme of the research and results included in the paper to attract their attention into reading the paper in full. The Table of Contents text **should be different from the abstract** and should be no more than 450 characters including spaces.))

A novel ^{11}C-labeled LRRK2 PET probe [^{11}C]**6** ([^{11}C]GNE-1023) was synthesized in good radiochemical yield, excellent radiochemical purity and high molar activity. Autoradiography studies demonstrated excellent in vitro specific binding of [^{11}C]**6** to LRRK2 in several species including rat and nonhuman primate brain tissues. The whole-body ex vivo bio-distribution studies exhibited limited brain accumulation, and excretion pathway, specifically urinary and hepatobiliary elimination for [^{11}C]**6** in mice. Nevertheless, further modification based on [^{11}C]**6** scaffold is necessary to improve the BBB permeability.